Universidade de São Paulo

Biblioteca Digital da Produção Intelectual - BDPI

Departamento de Física e Ciências Materiais - IFSC/FCM   Artigos e Materiais de Revistas Científicas - IFSC/FCM

2014-06

Nonuniversality of entanglement convertibility

Nonuniversality of entanglement convertibility

Helena Bragança,[1] Eduardo Mascarenhas,[1] G. I. Luiz,[1] C. Duarte,[2] R. G. Pereira,[3] M. F. Santos,[1] and M. C. O. Aguiar[1]

[1]*Departamento de Física, Universidade Federal de Minas Gerais, Belo Horizonte, MG, Brazil*
[2]*Departamento de Matemática, Universidade Federal de Minas Gerais, Belo Horizonte, MG, Brazil*
[3]*Instituto de Física de São Carlos, Universidade de São Paulo, C.P. 369, São Carlos, SP, 13560-970, Brazil*

Recently, it has been suggested that operational properties connected to quantum computation can be alternative indicators of quantum phase transitions. In this work we systematically study these operational properties in one-dimensional systems that present phase transitions of different orders. For this purpose, we evaluate the local convertibility between bipartite ground states. Our results suggest that the operational properties, related to nonanalyticities of the entanglement spectrum, are good detectors of explicit symmetries of the model, but not necessarily of phase transitions. We also show that thermodynamically equivalent phases, such as Luttinger liquids, may display different convertibility properties depending on the underlying microscopic model.

I. INTRODUCTION

Low-order phase transitions are directly related to singularities in the derivatives of the free energy, with such singularities marking the boundary between two macroscopically distinguishable phases. These transitions are usually described by Landau's paradigm of symmetry breaking and as such are detectable by local order parameters [1]. The singular behavior not only manifests itself in thermodynamical properties but also has dynamical consequences; for instance, the critical slowing down of adiabatic time evolution [2,3]. On the other hand, the existence of phase transitions that do not correspond to symmetry breaking is well established [4]. A simple example is provided by the infinite-order Berezinskii–Kosterlitz–Thouless (BKT) transition [5] realized in several two-dimensional systems at finite temperature, a recent example being cold atomic gases [6]. The BKT universality class also turns up in quantum phase transitions in one-dimensional (1D) systems such as spin chains [7] and Bose–Hubbard chains realizable in optical lattices [8]. The existence of such transitions and the growing interest in topological phases in general [9–14], which cannot be described by local order parameters, have motivated alternative approaches to address quantum phase transitions [15–17].

Quantum information theory has provided novel perspectives in this context based, for example, on the analysis of the intrinsic correlations (entanglement entropy, entanglement spectrum) of the quantum states of a given system [18–31]. More recently, a few studies have analyzed the so-called local convertibility of quantum states [10,32–34], which introduces an operational view related to quantum computation. This quantity is completely characterized by functions of the entanglement spectrum, either through majorization relations or the Rènyi entropies [35–38]. Remarkably, it has been shown that several phase transitions coincide with changes in the local convertibility [32–34].

In this work we analyze operational aspects of quantum systems by using the density matrix renormalization group (DMRG) technique. More concretely, we investigate the behavior of the local convertibility across several quantum phase transitions in one-dimensional spin-$\frac{1}{2}$ and spin-1 XXZ Hamiltonians. Our results show that changes of the local

convertibility typically correspond to points of symmetric Hamiltonians, which may not coincide with quantum phase transitions. We also give an example of an infinite-order (BKT) transition that is detached from *any* pre-existing symmetries, corresponding to *no* changes in the convertibility profile. Thus, according to our results the operational approach based on convertibility is a good detector of explicit symmetries rather than criticality. We clarify that the quantity we consider—the local convertibility—is related to a protocol of local operations, and our main conclusion is that this quantity indicates explicit symmetries of the Hamiltonians, whose generators are local operators (i.e., operators that are sums but never products of single-site operators). However, hidden symmetries, whose generators are nonlocal operators, are not directly detected by the convertibility, but through other properties of the entanglement spectrum.

II. LOCAL CONVERTIBILITY

Consider a quantum system described by a Hamiltonian H_λ, where λ is some tunable parameter. The system is partitioned into two subsystems, which are distributed to parties A and B. The two parties are given the task of converting the ground state $|\Psi_0^{(\lambda)}\rangle_{AB}$ of the initial Hamiltonian into $|\Psi_0^{(\lambda+\epsilon)}\rangle_{AB}$, the ground state of $H_{\lambda+\epsilon}$, by performing only local operations and classical communication (LOCC) on their respective subsystems. The general protocol allows for the use of an extra resource; namely, a shared ancillary entangled state called catalyst $|C\rangle$, with which they can freely operate, provided that $|C\rangle$ is left undisturbed at the end of the process, i.e., $|\Psi_0^{(\lambda)}\rangle |C\rangle \rightarrow |\Psi_0^{(\lambda+\epsilon)}\rangle |C\rangle$. This protocol is called local catalytic conversion [36–38].

The necessary and sufficient condition for catalytic conversion relies on the set of Rènyi entropies,

$$S_\alpha(\lambda) = \frac{1}{1-\alpha} \log \mathrm{Tr}[\rho_A^\alpha(\lambda)] = \frac{\log \sum_i [\xi_i(\lambda)]^\alpha}{1-\alpha}, \quad (1)$$

where $\rho_A(\lambda)$ is the reduced density matrix of subsystem A and $\xi_i(\lambda)$ are its eigenvalues which constitute the entanglement spectrum (ES) of the bipartition [23]. Note that S_0 is the logarithm of the rank of the state, i.e., the number of nonzero

eigenvalues of the reduced density matrix, and $S_{\alpha \to 1}$ is the von Neumann entropy or entanglement entropy (EE), while $S_{\alpha \to \infty}$ is the logarithm of the largest eigenvalue. The condition for conversion is $S_\alpha(\lambda) \geqslant S_\alpha(\lambda + \epsilon)$ for all α [37,38], i.e., no entropies can increase after the conversion. In the $\epsilon \to 0$ limit, this relation can be replaced by the analysis of the signs of the catalytic susceptibility $\chi(\alpha, \lambda) = \frac{\partial S_\alpha(\lambda)}{\partial \lambda}$. If $\chi < 0$ for all α, then conversion is only possible from λ to $\lambda + \epsilon$; if $\chi > 0$, $\forall \, \alpha$, then conversion is possible only in the opposite direction. For $\chi = 0$ conversion is possible in both directions. This criterium was used in Ref. [32] to analyze the power of adiabatic quantum computation in different phases of a given λ-parametrized Hamiltonian.

However, some states allow for local convertibility even in the absence of a catalyst. In this case one can use the criterium of majorization of quantum states, defined as [35]

$$M(j) = \frac{\partial}{\partial \lambda} \sum_{i=1}^{j} \xi_i(\lambda), \qquad (2)$$

where the entanglement spectrum is sorted in decreasing order. Convertibility from $|\Psi_0^{(\lambda)}\rangle$ to $|\Psi_0^{(\lambda+\epsilon)}\rangle$ in the absence of the catalyst is possible if $M(j) \geqslant 0$ for all j.

III. ANISOTROPIC SPIN-CHAIN MODELS

We consider the XXZ Hamiltonian

$$H = \sum_{l=1}^{N} \left[S_l^x S_{l+1}^x + S_l^y S_{l+1}^y + \Delta S_l^z S_{l+1}^z + D(S_l^z)^2 \right], \qquad (3)$$

where $\mathbf{S}_l^{(x,y,z)}$ are the spin operators at the lth site, Δ is the longitudinal nearest-neighbor exchange interaction, and D represents uniaxial single-ion anisotropy. In Eq. 3 and throughout this paper, we assume the transverse nearest-neighbor exchange interaction as the unit of energy. We study both spin-$\frac{1}{2}$ and spin-1 systems; for the former the single-ion anisotropy term is simply a constant since $(S^z)^2 = \frac{1}{4}$. We shall identify the control parameter λ with either Δ or D, depending on the transition in question. For any values of Δ and D, the model has an explicit U(1) rotational symmetry in the xy plane and a Z_2 spin inversion symmetry along the z axis.

The spin-$\frac{1}{2}$ model is integrable and exactly solvable by Bethe ansatz [7]. The system has two gapped phases: a ferromagnetic phase for $\Delta < -1$ and an antiferromagnetic (AFM) Néel phase for $\Delta > 1$, separated by a gapless Luttinger liquid (LL) XY phase for $-1 < \Delta \leqslant 1$. The phase transition between the ferromagnetic and LL phases is of first order, while the one between LL and AFM phases is a BKT transition. In the latter the gap decreases exponentially as $\Delta \to 1^+$, which poses a challenge for numerical techniques attempting to detect the critical point [27,39]. The model has an explicit SU(2) symmetry at $\Delta = 1$ (both in the spin-$\frac{1}{2}$ and spin-1 cases); that is, there exists a set of four operators $Z = \sum_l S_l^z$ (the total Z spin), S^2 (the total spin), $Q_L^- = \sum_l S_l^- = \sum_l (S_l^x - i S_l^y)$ (a lowering operator), and $Q_L^+ = \sum_l S_l^+ = \sum_l (S_l^x + i S_l^y)$ (a raising operator) which commute with the Hamiltonian at $\Delta = 1$ and are constructed as sums over local operators.

The spin-1 model is not integrable, but its ground state phase diagram is known [40,41]. Let us first focus on the

$D = 0$ line. In this case one finds a ferromagnetic phase for $\Delta \leqslant -1$, a LL XY phase for $-1 < \Delta \leqslant 0$, a Haldane phase for $0 < \Delta \lesssim 1.18$, and a Néel phase for $\Delta \gtrsim 1.18$ [42,43]. The gapped Haldane phase is characterized by a nonlocal string order parameter that breaks a hidden $Z_2 \times Z_2$ symmetry [44] and is an example of a symmetry-protected topological phase [12]. Most interestingly, the transition between the XY and the Haldane phase is of BKT type and is known to occur exactly at $\Delta = 0$ due to a hidden SU(2) symmetry generated by nonlocal operators [45]. To be more specific, in this case the Q_{NL} operators that define the algebra satisfy

$$Q_{NL}^+ = \sum_j (S_j^+)^2 e^{i\pi \sum_{l<j} S_l^z},$$

$$Q_{NL}^- = \sum_j (S_j^-)^2 e^{i\pi \sum_{l<j} S_l^z},$$

$$Q_{NL}^z = \frac{1}{2}[Q_{NL}^+, Q_{NL}^-];$$

that is, they involve sums over nonlocal operators, in contrast to the case of the explicit SU(2) symmetry present at $\Delta = 1$.

Switching on the single-ion anisotropy in the spin-1 model gives rise to a BKT transition line in the phase diagram [42]. While the transition between XY and Haldane remains pinned at $\Delta = 0$ due to the hidden SU(2) symmetry, there appears a BKT transition between the XY phase and a so-called large-D phase, favored by strong easy-plane anisotropy ($D > 0$). The gapped large-D phase is topologically trivial because the nondegenerate ground state is adiabatically connected to the product state with $S_l^z = 0$ for all spins. The transition from XY to large D is completely dissociated from high-symmetry points in the lattice model. It is important to distinguish between the exact SU(2) symmetry at $\Delta = 0$ [45] and the SU(2) symmetry that arises in the renormalization group analysis of the sine-Gordon model, which is the effective field theory for the BKT transition [46,47]. This emergent symmetry is a genuine signature of a quantum phase transition since it becomes asymptotically exact in the thermodynamic limit.

IV. RESULTS

A. Operational properties

For both spin-$\frac{1}{2}$ and spin-1 models, the ground state is always one of the two degenerate fully polarized states for any $\Delta \leqslant -1$. Thus, in the ferromagnetic phase $\chi = 0$ and convertibility is possible between any two points (in both directions).

The other phases have nontrivial convertibility behavior. First consider the spin-$\frac{1}{2}$ model. In the left panels of Fig. 1 we present the sign of the catalytic susceptibility obtained by using DMRG for open chains with $N = 112$ sites (top panels) and $N = 212$ (bottom panels). Differently from the ferromagnetic phase, for $-1 < \Delta < 1$ (which corresponds to the critical LL phase in the thermodynamic limit), $\chi < 0$ for all α, which indicates unidirectional convertibility. In addition, the convertibility changes direction at the isotropic point $\Delta = 1$. The convertibility is then lost (i.e., the sign of χ depends on α) as Δ increases and it is recovered (unidirectionally) for larger Δ as the ground-state approaches the classical Néel state. The
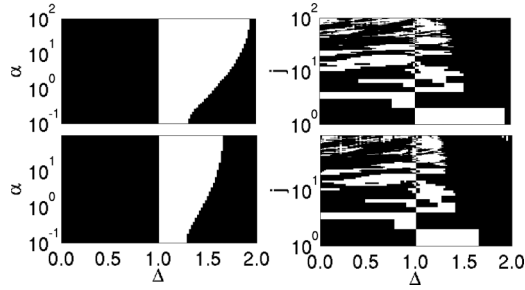
FIG. 1. (left panels) The sign of the catalytic susceptibility χ for different Rènyi entropies and (right panels) majorization M as a function of Δ for a spin-$\frac{1}{2}$ chain with (top panels) $N = 112$ and (bottom panels) $N = 212$, where N is the size of the chain. The black regions indicate $\chi < 0$ (or $M < 0$) and the white regions correspond to $\chi > 0$ (or $M > 0$). The data were generated for a symmetrical bipartite system $A = B = N/2$, retaining 100 states at the DMRG calculation, which keeps the truncation error below 10^{-9}.
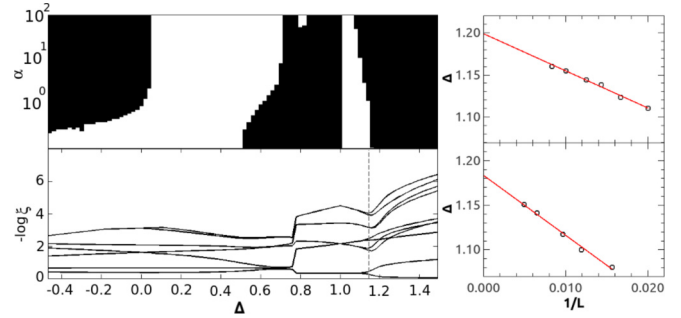

FIG. 2. (Color online) (top-left panel) Sign of the catalytic susceptibility for different Rènyi entropies and (bottom-left panel) entanglement spectrum of a symmetrical bipartite $A = B = N/2$ spin-1 system as a function of Δ, for $D = 0$ and $N = 106$. The right panels show finite-size scaling procedures corresponding to the point where (top panel) the unidirectional convertibility is recovered and (bottom panel) the level degeneracies are lifted when going from the Haldane phase to the Néel phase.

convertibility is sensitive to the chain length: the larger the system, the smaller the value of Δ for which it presents the convertibility characteristic of strong AFM behavior.

Results for the majorization analysis are shown in the right panels of Fig. 1 for both $N = 112$ and $N = 212$, from which we can see that the use of a catalyst in the conversion is dispensable only in the strong AFM regime.

We stress that, independently of the chain length, the catalytic convertibility changes direction exactly at the Heisenberg point $\Delta = 1$ (see Fig. 1), which coincides with the SU(2) symmetry of the model. The absence of finite-size effects at this point, even for small chains with $N \sim 10$ sites, suggests that the convertibility is detecting the SU(2) symmetry (expected to be present for chains of *any* size), rather than the phase transition, whose precursors should be apparent only for large systems. It is also interesting that the majorization relations (also in Fig. 1) display a local mirror-like symmetry around $\Delta = 1$, which reinforces that these quantities detect the SU(2) symmetry.

Let us now discuss the $D = 0$ spin-1 model. Our results for the convertibility properties in this case are presented in the top panels of Fig. 2. Interestingly, the LL phase ($-1 < \Delta < 0$) is not locally convertible, since the sign of χ depends on α, unlike the LL phase in the spin-$\frac{1}{2}$ model, which is convertible. This is a remarkable fact: even though the LL phases of spin-$\frac{1}{2}$ and spin-1 models share the same low-energy physics, they exhibit different operational behavior. Nevertheless, we note that the catalytic susceptibilities corresponding to large values of α, which are dominated by the largest eigenvalues of the density matrix, have the same sign ($\chi < 0$) for both spin-$\frac{1}{2}$ and spin-1 LL phases. This seems consistent with the general expectation that universal information can be extracted from the low-lying levels in the ES [23,25]. In contrast, the low-α (i.e., "high temperature" [23]) susceptibilities may depend on details of the microscopic model.

Now, the transition from the LL to the Haldane phase (known to occur at $\Delta = 0$ in the thermodynamic limit) does not coincide with a change in the convertibility (see Fig. 2). At this point the Hamiltonian presents the hidden SU(2) symmetry (related to *nonlocal* operators) discussed previously in this

paper. This *hidden* symmetry is not detected by the *local* convertibility. Nonetheless, it is important to stress that the EE ($S_{\alpha \to 1}$) does present a derivative that changes sign exactly at the symmetry point, which also coincides with a level crossing in the ES (bottom of the figure). For $\alpha < 1$, the susceptibilities change sign for $\Delta < 0$, while for $\alpha > 1$ the sign changes happen for $\Delta > 0$. Thus, even though the convertibility is blind to this hidden symmetry, it is still encoded in the ES.

Figure 2 (top-left panel) also shows changes in the convertibility profile within the Haldane phase. The unidirectional convertibility is established approximately once the phase is reached ($0 \lesssim \Delta \lesssim 0.5$), but it is then lost for $0.5 \lesssim \Delta \lesssim 0.7$. As Δ increases even further, still in the Haldane phase, the convertibility is recovered in the opposite direction. More interestingly, χ changes sign for all α exactly at the SU(2) symmetry point $\Delta = 1$. We emphasize that all these alterations happen inside the same phase, leading us to conclude that changes in the local convertibility do not necessarily correspond to phase transitions. In fact, previous works have shown that nonanalyticities in the EE do not necessarily correspond to real phase transitions but can, for instance, separate a commensurate and an incommensurate phase [48]. Furthermore, in the present work we show that there seems to be a direct relation between the behavior of the local convertibility and symmetries related to local operators.

The convertibility profile is a function of the ES. The ten largest eigenvalues of the reduced density matrix are presented in the bottom panel of Fig. 2. As we can see, the most abrupt changes in the convertibility properties occur in the vicinity of points of either level crossing (e.g., near $\Delta = 1$) or degeneracy breaking of the ES (e.g., near $\Delta \approx 1.18$); that is, are related to nonanalyticities of the ES.

It is interesting to understand why there are level crossings at $\Delta = 0$ and $\Delta = 1$, which correspond to the SU(2) symmetry points. The system ground state is an eigenvector of the symmetry operators and the partition we consider does not break the symmetry. This means that the left and right eigenvectors of the Schmidt decomposition can be identified by the symmetry quantum numbers. For the SU(2) symmetry,

energy eigenvectors corresponding to different eigenvalues of S_z can be degenerate if they are connected by the S^+ or S^- operators defined at each partition. This gives rise to the level crossings we observe in Fig. 2. Because these crossings are associated with the symmetry, which is present for systems of any size, we do not expect these crossings to shift with the system size, as is indeed observed in our numerical results (not shown). We add that the connection between symmetry and nonanalyticities in the EE or degeneracy in the ES has been analyzed in detail in other cases [24,49]. We stress that, even though the ES and the EE are sensitive to both symmetric points $\Delta = 1$ and $\Delta = 0$, the local convertibility captures the explicit symmetry (present at $\Delta = 1$) whose generators are local operators, but not the hidden one (at $\Delta = 0$ whose generators are nonlocal).

A second-order (Ising type) phase transition from the Haldane to the Néel phase happens for $\Delta \approx 1.18$ (in the thermodynamic limit) [42,43]. As can be seen in the top-left panel of Fig. 2, around this value of Δ we observe a change in the convertibility sign. Contrary to the cases we analyze above, here the convertibility profile *is* sensitive to finite-size effects. Note that this phase transition falls under the standard symmetry breaking paradigm and, if the convertibility is able to detect the transition, it should depend on the system size, as indeed it does.

In previous literature [32,34], changes in the convertibility profile are associated with this symmetry-breaking type of transition, but only small systems are analyzed (up to 18 sites). Here we consider larger systems and perform a finite-size scaling analysis, which can be seen at the top-right panel of Fig. 2. In the thermodynamic limit, the critical Δ obtained from our scaling procedure is $\Delta \approx 1.20$, which slightly deviates from the known value of $\Delta \approx 1.18$. Indeed, we do not expect a very good estimate of the critical Δ from the convertibility, since the changes in its profile correspond to Rènyi entropies of small α that strongly depend on the smallest reduced-density-matrix eigenvalues, which intrinsically have less accuracy in the DMRG calculation.

The largest eigenvalues of the reduced density matrix are numerically more precise and indeed the ten largest of them can be used to better determine where this Ising type of transition happens. The change in the convertibility analyzed above corresponds to a level splitting in the ES—see the dashed line in the bottom-left panel of the figure. This degeneracy breaking can be associated with the Haldane–Néel phase transition since for open chains the higher degeneracy of the Haldane phase is attributed to the spontaneous breaking of the hidden $Z_2 \times Z_2$ symmetry [24]. The value of Δ where this degeneracy is lifted also *shifts* with the system size and a finite-size scaling allows us to obtain the corresponding value in the thermodynamic limit. As can be seen in the bottom-right panel of Fig. 2, our analysis yields $\Delta \approx 1.18$, in good agreement with the known critical value for the Haldane–Néel phase transition [42,43].

We are thus able to correctly identify the transition point by analyzing the ES, which is directly related to the convertibility profile. This result and the previous literature suggest that the convertibility is a detector of criticality only in the case of transitions associated with symmetry breaking. In most of the cases, however, it is a detector of explicit symmetries of the Hamiltonian.
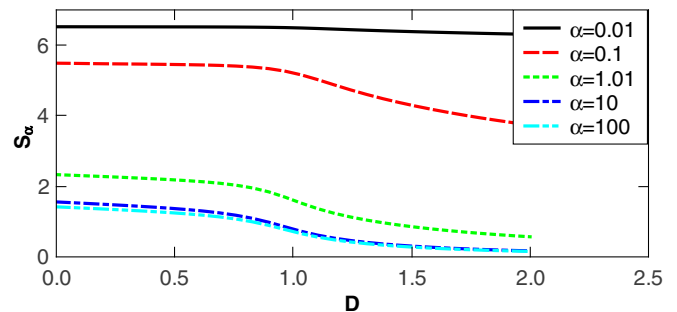

FIG. 3. (Color online) Rènyi entropies S_α ($\alpha = 0.01, 0.1, 1.01,$ 10, and 100) for a $N = 206$, spin-1 chain with fixed $\Delta = -0.5$ and $A = B = N/2$, as a function of D. The entropies are always monotonic, which means that there is no change in the direction of the convertibility.

Regarding the majorization relations, our results for the spin-1 system indicate that convertibility without a catalyst is possible only in the strong-AFM (large Δ) regime, similarly to the Néel phase of the spin-$\frac{1}{2}$ model.

B. Single-ion anisotropy

To strengthen the conclusion drawn above that the convertibility is a detector of symmetries instead of phases transitions, we study the spin-1 XXZ chain with single-ion anisotropy. As mentioned above, the phase diagram for $\Delta < 0$ and $D > 0$ contains a BKT transition (without symmetry breaking) from a critical XY phase to a gapped large-D phase [41]. This transition does not coincide with any high-symmetry points in the Hamiltonian for finite chains. In Fig. 3, we show results for some Rènyi entropies as a function of positive D, for $\Delta = -0.5$. The main point is that all entropies decrease monotonically with D, leading to a uniform convertibility profile ($\chi < 0$ for all α and all D). The BKT transition is expected to happen at $D \approx 0.8$ for $\Delta = -0.5$ [41], but there is no sign of it in the convertibility profile. We stress that this is the first example (to our knowledge) of a phase transition around which there is absolutely no change in the convertibility.

C. Critical entanglement entropy

The phase transition analyzed in the last section constitutes an important example in the context of our work, since it is not accompanied by a change in the convertibility. This infinite-order phase transition which does not have a pre-existing SU(2) symmetry has, however, a small amount of work dedicated to it. Here we show that the EE $S_{\alpha \to 1}$ can be used to detect it through a simple finite-size analysis.

In Fig. 4 we show the EE, $S(x)$, as a function of the partition size x for $N = 106$, $\Delta = -0.5$ and different values of the single-ion anisotropy D. It is clear that the behavior of $S(x)$ qualitatively changes with D: it increases logarithmically with x for small D, but saturates for large D values, indicating a phase transition.

In fact, the EE is especially useful since it has been shown to exhibit universal scaling in the LL phase, which is described by a conformal field theory (CFT) with central charge $c = 1$. Using CFT, Calabrese and Cardy [50] showed that the EE of a finite system with open boundary conditions (OBCs) in the
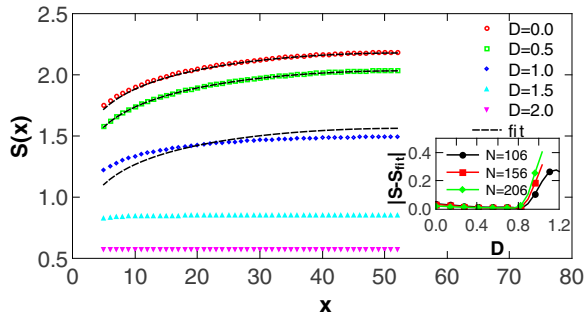
FIG. 4. (Color online) Entanglement entropy as a function of the partition size x for $N = 106$, $\Delta = -0.5$ and different values of the single-ion anisotropy D. The fittings of the numerical data to Eq. 4 are also shown. The inset presents the fitting accuracy for systems of three sizes ($N = 106, 156, 206$), from which we find the BKT critical point at $D \approx 0.8$.

regime $x, N \gg 1$ is given by

$$S(x, N) = \frac{c}{6} \log \left[\frac{2N}{\pi} \sin \left(\frac{\pi x}{N} \right) \right] + s', \tag{4}$$

where s' is a nonuniversal constant.

We can find the BKT critical point by fitting the numerical data to Eq. 4, leaving c and s' as free parameters, as shown in Fig. 4. For small D, the numerical data are well fit by Eq. (4), indicating that the system is in the critical phase. As D increases, however, the behavior of $S(x)$ starts to deviate from the CFT prediction. The fitting accuracy (inset of the figure) clearly shows that Eq. (4) correctly describes the EE for $D \lesssim 0.8$, leading us to estimate that the BKT critical point is at $D = 0.82 \pm 0.07$, in accordance with previous results [41]. Inside the critical region, the values of the free parameters are as expected: s' is independent of the chain length and $c \approx 1$.

V. CONCLUSIONS

The local convertibility of many-body quantum states, an important concept in quantum information and computation theory, provides a comparison of the computational potential of adiabatic and LOCC procedures. The results presented in this paper strongly suggest that this operational perspective on quantum states is not necessarily related to quantum phase transitions, but reflects properties of the entanglement spectrum which are intimately connected with symmetries of the microscopic model. In fact, we explicitly showed examples of local convertibility changes that do not correspond to phase transitions and phase transitions that do not correspond to alterations of the local convertibility. Furthermore, different models that fall into the same universality class, such as Luttinger liquids, may exhibit distinct convertibility properties. Hence, the nonuniversality of the convertibility.

Upon preparation of this manuscript we became aware of Ref. [51], where the entanglement spectrum for a couple of systems is shown to display pseudotransitions that do not correspond to physical phase transitions. The authors then conclude that it may be misleading to use entanglement measurements as detectors of quantum phase transitions, in agreement with our conclusions. Note that their conclusions are based on a different approach than ours; that is, one not related to high-symmetry points or operational aspects.

[1] S. Sachdev, *Quantum Phase Transitions* (Cambridge University Press, Cambridge, 1999).

[2] A. Polkovnikov, Phys. Rev. B **72**, 161201(R) (2005).

[3] P. Doria, T. Calarco, and S. Montangero, Phys. Rev. Lett. **106**, 190501 (2011); T. Caneva, T. Calarco, R. Fazio, G. E. Santoro, and S. Montangero, Phys. Rev. A **84**, 012312 (2011).

[4] X.-G. Wen, *Quantum Field Theory of Many-Body Systems* (Oxford University Press, Oxford, 2007).

[5] V. L. Berezinskii, Zh. Eksp. Teor. Fiz. **61**, 1144 (1972) [Sov. Phys. JETP **34**, 610 (1972)]; J. M. Kosterlitz and D. J. Thouless, J. Phys. C **6**, 1181 (1973).

[6] C.-L. Hung, X. Zhang, N. Gemelke, and C. Chin, Nature (London) **470**, 236 (2011).

[7] T. Giamarchi, *Quantum Physics in One Dimension* (Claredon Press, Oxford, 2004).

[8] Maciej Lewenstein, Anna Sanpera, and Veronica Ahufinger, *Ultra Cold Atoms in Optical Lattices* (Oxford University Press, Oxford, 2012).

[9] A. Hamma and D. A. Lidar, Phys. Rev. Lett. **100**, 030502 (2008).

[10] A. Hamma, L. Cincio, S. Santra, P. Zanardi, and L. Amico, Phys. Rev. Lett. **110**, 210602 (2013).

[11] P. Bonderson and C. Nayak, Phys. Rev. B **87**, 195451 (2013).

[12] F. Pollmann and A. M. Turner, Phys. Rev. B **86**, 125441 (2012).

[13] Y. Zhao, W. Li, B. Xi, Z. Zhang, X. Yan, S.-J. Ran, T. Liu, and G. Su, Phys. Rev. E **87**, 032151 (2013).

[14] Z.-X. Liu, X. Chen, and X.-G. Wen, Phys. Rev. B **84**, 195145 (2011).

[15] X. Chen, Z.-C. Gu, and X.-G. Wen, Phys. Rev. B **84**, 235128 (2011).

[16] N. Schuch, D. Perez-Garcia, and I. Cirac, Phys. Rev. B **84**, 165139 (2011).

[17] Y. H. Su, B.-Q. Hu, S.-H. Li, and S. Y. Cho, Phys. Rev. E **88**, 032110 (2013).

[18] Y. Zhang, T. Grover, and A. Vishwanath, Phys. Rev. Lett. **107**, 067202 (2011).

[19] L. Amico, R. Fazio, A. Osterloh, and V. Vedral, Rev. Mod. Phys. **80**, 517 (2008).

[20] A. Osterloh, L. Amico, G. Falci, and R. Fazio, Nature (London) **416**, 608 (2002); G. Vidal, J. I. Latorre, E. Rico, and A. Kitaev, Phys. Rev. Lett. **90**, 227902 (2003).

[21] E. Mascarenhas, L. Heaney, M. C. O. Aguiar, and M. F. Santos, New J. Phys. **14**, 043033 (2012).

[22] C. Mund, O. Legeza, and R. M. Noack, Phys. Rev. B **79**, 245130 (2009).

[23] H. Li and F. D. M. Haldane, Phys. Rev. Lett. **101**, 010504 (2008).

[24] F. Pollmann, A. M. Turner, E. Berg, and M. Oshikawa, Phys. Rev. B **81**, 064439 (2010).

[25] P. Calabrese and A. Lefevre, Phys. Rev. A **78**, 032329 (2008).

[26] R. Thomale, A. Sterdyniak, N. Regnault, and B. A. Bernevig, Phys. Rev. Lett. **104**, 180502 (2010).

[27] M. Goldstein, Y. Gefen, and R. Berkovits, Phys. Rev. B **83**, 245112 (2011).

[28] V. Alba, M. Haque, and A. M. Läuchli, Phys. Rev. Lett. **108**, 227201 (2012).

[29] G. De Chiara, L. Lepori, M. Lewenstein, and A. Sanpera, Phys. Rev. Lett. **109**, 237208 (2012).

[30] L. Lepori, G. De Chiara, and A. Sanpera, Phys. Rev. B **87**, 235107 (2013).

[31] S. M. Giampaolo, S. Montangero, F. Dell Anno, S. De Siena, and F. Illuminati, Phys. Rev. B **88**, 125142 (2013).

[32] J. Cui, M. Gu, L. C. Kwek, M. F. Santos, Heng Fan, and V. Vedral, Nat. Commun. **3**, 812 (2012).

[33] J. Cui, L. Amico, H. Fan, M. Gu, A. Hamma, and V. Vedral, Phys. Rev. B **88**, 125117 (2013).

[34] J. Cui, J. P. Cao, and H. Fan, Phys. Rev. A **85**, 022338 (2012).

[35] M. A. Nielsen, Phys. Rev. Lett. **83**, 436 (1999).

[36] D. Jonathan and M. B. Plenio, Phys. Rev. Lett. **83**, 3566 (1999).

[37] S. Turgut, J. Phys. A: Math. Theor. **40**, 12185 (2007).

[38] Y. R. Sanders and G. Gour, Phys. Rev. A **79**, 054302 (2009).

[39] K. Okamoto and K. Nomura, J. Phys. A: Math. Gen. **29**, 2279 (1996).

[40] M. den Nijs and K. Rommelse, Phys. Rev. B **40**, 4709 (1989).

[41] W. Chen, K. Hida, and B. C. Sanctuary, Phys. Rev. B **67**, 104401 (2003).

[42] M. Tsukano and K. Nomura, J. Phys. Soc. Jpn. **67**, 302 (1998).

[43] Y. H. Su, S. Y. Cho, B. Li, H.-L. Wang, and H.-Q. Zhou, J. Phys. Soc. Jpn. **81**, 074003 (2012).

[44] T. Kennedy and H. Tasaki, Phys. Rev. B **45**, 304 (1992).

[45] A. Kitazawa, K. Hijii, and K. Nomura, J. Phys. A: Math. Gen. **36**, L351 (2003).

[46] T. Giamarchi and H. J. Schulz, Phys. Rev. B **39**, 4620 (1989).

[47] K. Nomura and A. Kitazawa, J. Phys. A: Math. Gen. **31**, 7341 (1998).

[48] Ö. Legeza, J. Sólyom, L. Tincani, and R. M. Noack, Phys. Rev. Lett. **99**, 087203 (2007).

[49] E. H. Kim, Ö. Legeza, and J. Sólyom, Phys. Rev. B **77**, 205121 (2008).

[50] P. Calabrese and J. Cardy, J. Stat. Mech. (2004) P06002.

[51] A. Chandran, V. Khemani, and S. L. Sondhi, arXiv:1311.2946.